Available online at www.sciencedirect.com
SCIENCE DIRECT®
Journal of Physics and Chemistry of Solids 66 (2005) 1370–1375
JOURNAL OF PHYSICS AND CHEMISTRY OF SOLIDS
www.elsevier.com/locate/jpcs

Spectroscopic imaging STM studies of high-T_C superconductivity

Jinho Lee, James A. Slezak, J.C. Davis*

LASSP, Department of Physics, Cornell University, Ithaca, NY 14853, USA

Abstract

Since its discovery in 1986, understanding both the ground state and excited states of high temperature superconductivity (HTSC) has been one of the main challenges in modern condensed matter physics. One remarkable observation in HTSC cuprates is that the superconductivity appears as the localized electrons of a Mott insulator become itinerant due to carrier doping. Momentum sensitive probes like Angle Resolved Photo-Emission Spectroscopy (ARPES) and Inelastic Neutron Scattering (INS) have played important roles in mapping the momentum-space properties of the cuprate electronic structure. However, considering that cuprate superconductivity develops from atomically localized electrons and shows nanoscale disorder, a purely momentum dependent description is far from sufficient. Here, we describe novel spectroscopic imaging scanning tunneling microscopy (SI-STM) studies, which can probe the real-space electronic structure at the nano-scale, along with momentum-space electronic structure. We discuss a series of recent results from SI-STM studies of $Bi_2Sr_2CaCu_2O_{8+x}$ and $Ca_{2-x}Na_xCuO_2Cl_2$.

Keywords: A. Superconductors; C. Scanning tunneling microscopy; D. Electronic structure

1. Introduction

According to the BCS theory, the degenerate electron gas can be unstable against pairing of electrons with opposite spin and momentum, if an attractive electron–electron interaction potential exists [1]. The condensation of these Cooper pairs leads to the superconducting ground state. In conventional superconductors, the pairing potential has typically s-wave symmetry. In the superconducting state, a gap forms in the density of states (DOS) of electrons. Virtually no electronic states are available inside of this superconducting gap at zero temperature. Outside of this gap, new excited states called Bogoliubov quasiparticles appear. These 'dressed-electron' states near the Fermi level have a DOS and dispersion-relation dramatically different from those of electrons in the normal metallic state. We can use scanning tunneling spectroscopy to measure the directly local density of states of the Bogoliubov quasiparticles. Also, using the STM's spatial resolution ~ 1 Å, we can get information about local variations of DOS (LDOS). This is possible at low temperature when vibrational and acoustic noise is greatly diminished [2].

2. Mott insulator to high-T_C

There are many cuprate high-T_C superconductors falling into families of structures with different numbers of immediately adjacent Cu–O planes. $La_{2-x}X_xCuO_4$(X = Ba^{2+}, Sr^{2+}, Ca^{2+} etc.), $YBa_2Cu_3O_{6+x}$, $Bi_2Sr_2CaCu_2O_{8+x}$, and $Tl_2Ba_2Ca_2Cu_3O_{10}$, $HgBa_2Ca_3Cu_4O$, and recent $Ca_{2-x}Na_xCuO_2Cl_2$ (chronological order of discoveries) are among the most studied [3]. Both experimentalists and theorists agree that superconductivity and charge transport are confined to the CuO_2 planes. The Cu atoms are believed to be in the $Cu^{2+}3d^9$ configuration with spin half. As shown in Fig. 1A, the dominating electronic state is an anti-ferromagnetic Mott insulator due to the fact that strong Coulomb repulsion prevents electron hopping from Cu to Cu, and because the anti-ferromagnetic order is energetically favorable.

As we remove some spins from these sites, hopping of electrons between Cu and Cu becomes possible (Fig. 1B). In this fashion, new electronic ordered states emerge as we dope the insulating CuO_2 layer with holes or electrons. High temperature superconductivity is one of them. These

* Corresponding author.
E-mail address: jcdavis@ccmr.cornell.edu (J.C. Davis).

0022-3697/$ - see front matter © 2005 Elsevier Ltd. All rights reserved.
doi:10.1016/j.jpcs.2005.05.073

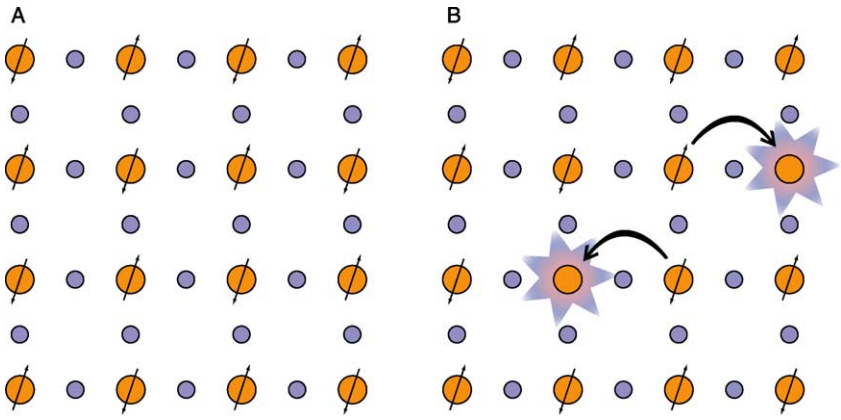

Fig. 1. A cartoon for the relevant electronic degrees of freedom in the CuO_2plane of the cuprates. Orange circles are the Cu atoms. (A) Square lattice with one spin half state at every vertex. Coulomb repulsion prevents hopping and antiferromagnetic (AF) correlations impose an overall AF ground state. (B) After removing 12.5% of spins in this figure, hopping of electrons becomes possible.

high-T_C superconductors have many physical properties different from the conventional superconductors. Pairing symmetry of cuprates is believed to exhibit $d_{x^2-y^2}$ symmetry [4,5], compared to s-wave like pairing symmetry in conventional superconductors. The highly anisotropic critical current (J_C), very high critical field (H_C), and the short coherence length (ξ) are all extremely different from conventional superconductors. Especially significant is that almost all the physical length scales are $\sim$1 nm: Cu–Cu distance is around 0.38 nm, superconducting coherence length ξ is 1–2 nm, inter-dopant atomic distance L$\sim$1.5 nm, and the Fermi wavelength $\lambda_F \sim 1$ nm. These similar length scales imply that different electronic phenomena can interact strongly with each other, unlike in usual metals where those length scales differ by orders of magnitudes. A typical schematic phase diagram of the hole-doped high-T_C cuprates is shown in Fig. 2. Around the hole doping level (p) of 0.16, T_C reaches its maximum value. One interesting thing about this diagram is that a mysterious 'pseudogap' phase [6] exists below the line T^*, above the superconducting dome.

3. Spectroscopic imaging STM (SI-STM)

We have developed several novel spectroscopic imaging techniques to investigate these highly complicated materials. First, atomic resolution local density of states (LDOS) imaging was introduced to cuprates [7]. To make energy-resolved LDOS maps, we measure differential conductance $g(\vec{r},V) \equiv (\mathrm{d}I/\mathrm{d}V)|_{\vec{r},V}$ between the STM tip and the sample, with spatial ($\vec{r}$) resolution $\sim$Å/pixel, and energy resolution $\sim$1 meV /point. Due to the relation LDOS$(\vec{r},E=eV) \propto g(\vec{r},V)$, this map is actually a spatial image of the LDOS at energy E : LDOS$(\vec{r},E)$. Second, we introduced the concept of the *gap map* where the spatial dependence of the superconducting gap value $\Delta(\vec{r})$ is mapped out with atomic resolution [8]. Yet another technique we recently developed for cuprate studies is Fourier Transform Scanning Tunneling Spectroscopy (FT-STS) [9]. To achieve FT-STS, one needs large field of view (FOV), as well as high resolution LDOS$(\vec{r},E)$ map to get good resolution in k-space, and at the same time a |k|-range up to the first brillouin zone. After performing 2D-FFT (Fast Fourier Transform) of LDOS$(\vec{r},E)$, we can identify $\vec{q}$-vectors of spatial modulations in LDOS$(\vec{r},E)$ by the locations of peaks in LDOS$(\vec{k},E)$-the Fourier transform magnitude of LDOS$(\vec{r},E)$. This technique has been exceptionally fruitful [10] in relating the atomic-scale $\vec{r}$-space electronic structure to that in $\vec{k}$-space. Finally, a fourth technique is atomically registered LDOS subtraction, wherein the perturbations to the background LDOS by an external magnetic field can be determined even in a strongly disordered environment by subtracting the original LDOS measured before application of the field [11].

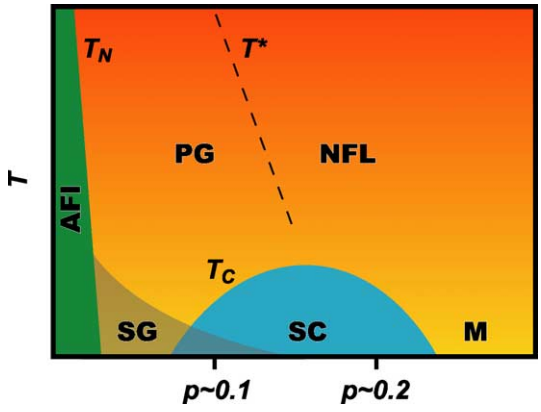

Fig. 2. Phase diagram for the cuprates as a function of temperature and hole doping. Phases with abbreviations are anti-ferromagnetic insulating (AFI), the pseudogap (PG), non-Fermi liquid (NFL), spin glass (SG), superconducting (SC) and metallic (M). The line labeled as T^* designates pseudogap transition line.

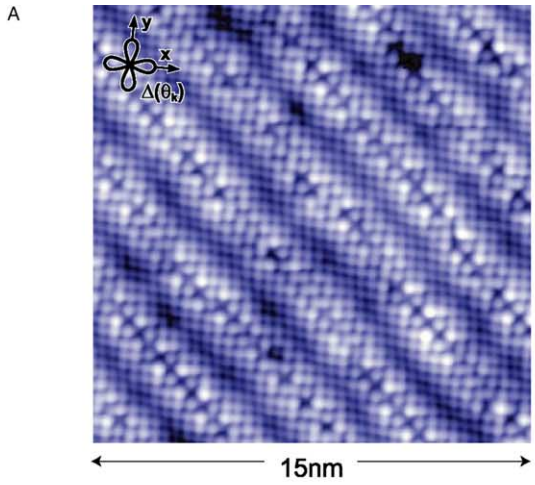

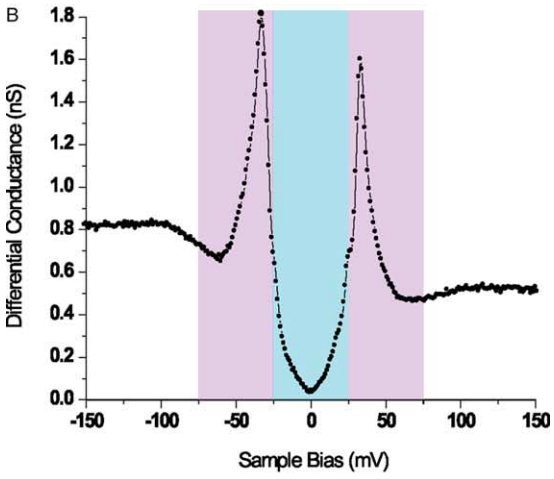

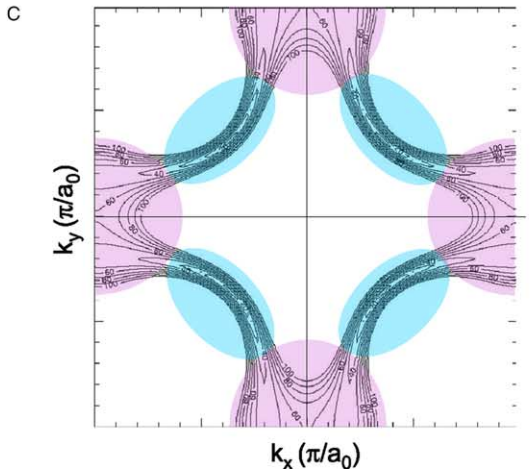

Fig. 3. (A) topographic image of a 150×150 Å field of view (FOV) of the BiO surface of $Bi_2Sr_2CaCu_2O_{8+x}$. Supermodulation with ∼26 Å periodicity, as well as the atomic grid are visible. (B) A typical form for the measured LDOS at a point on this surface, with two energy regions colored differently. (C) The $\vec{k}$-space contours of constant energy in superconducting state, identifying states in space that have the same energy.

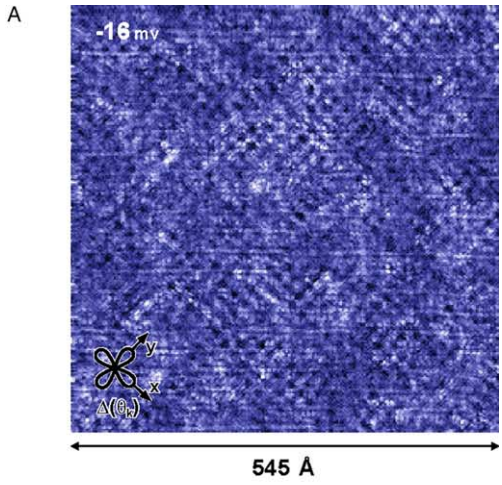

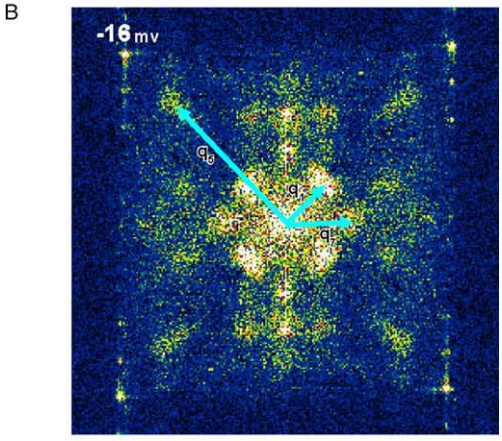

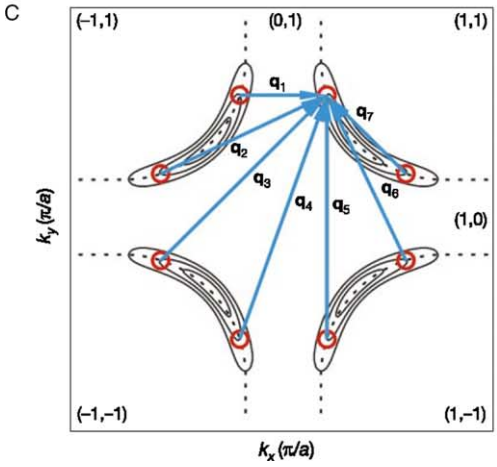

Fig. 4. (A) Quasiparticle interference modulations in LDOS map of $Bi_2Sr_2CaCu_2O_{8+x}$ at −16 meV. (B) The Fourier transform of this map $g(\vec{q}, E = -12$ meV), with several $\vec{q}$-vectors identified with arrows. (C) The quasiparticle interference model: wavevectors (blue) connect points of high DOS (low $|\nabla E|$) on a contour of constant energy. The normal state Fermi surface is given by dashed lines.

4. Local density of states spectrum in $Bi_2Sr_2CaCu_2O_{8+x}$

$Bi_2Sr_2CaCu_2O_{8+x}$ single crystals can cleave easily at the weakest link between BiO layers to reveal a relatively flat BiO surface. Therefore, the CuO_2 plane is only 5 Å below from the top surface, separated from the tip by insulating BiO and SrO layers which act to protect the CuO_2 plane of interest. Partly due to this remarkable property, most of the studies described here have been performed on $Bi_2Sr_2CaCu_2O_{8+x}$. The Cu atoms are located about 5 Å below Bi atoms. Fig. 3A shows a topographic image of a 150 Å square field of view (FOV) of the BiO surface. A clear Bi atomic grid can be seen, but no O atoms are visible due to their LDOS vanishing near E_F. The appearance of dark and bright spots is a real effect of the nanoscale inhomogeneity in superconducting $Bi_2Sr_2CaCu_2O_{8+x}$ [12,13] and not from surface damage. Also along the *b*-axis, a three-dimensional supermodulation [14] of ~26 Å produces brighter corrugations of the surface, which is due to the vertical displacement of the atoms from their ideal orthorhombic lattice sites. As mentioned, $Bi_2Sr_2CaCu_2O_{8+x}$ is believed to show $d_{x^2-y^2}$ like pairing potential (gap) symmetry [4,5]. A typical LDOS spectrum measured on the BiO plane of optimally doped $Bi_2Sr_2CaCu_2O_{8+x}$ is shown in Fig. 3B. This form of function is the central observable of our studies, revealing many of the attributes expected for the $d_{x^2-y^2}$ gap structure. We can immediately point out two energy regions of interest, as colored blue and purple, respectively. The same color scheme is used in Fig. 3C, indicating the regions of the 'contours of constant energy (CCE)' in momentum-space associated with the two energy ranges of Fig. 3B: $|E| <$ 25 meV and 25 meV $\leq |E| \leq$ 75 meV. Also in Fig. 3C, $d_{x^2-y^2}$ superconducting band structure [15] is illustrated in which CCE are plotted in $\vec{k}$-space.

5. LDOS modulations in low energies

At energies $|E| < 25$ meV, complex patterns of modulations appear in LDOS of $Bi_2Sr_2CaCu_2O_{8+x}$. The wavelengths of these modulations are of the order of several unit cells as shown in Fig. 4A. To find the wave vectors associated with these patterns, 2D-FFT analysis proved to be very useful. In Fig. 4B, sets of clearly discernible wave vectors are shown. The brightest spots in the corners in Fig. 4B are the 2D-*Bragg* peaks. 16 sets of $\vec{q}$'s have been identified and some of them are illustrated in Fig. 4C [10]. Since we carry out this process as a function of electron energy *E*, we dubbed this analysis as Fourier Transform Scanning Tunneling Spectroscopy (FT-STS). As we analyze

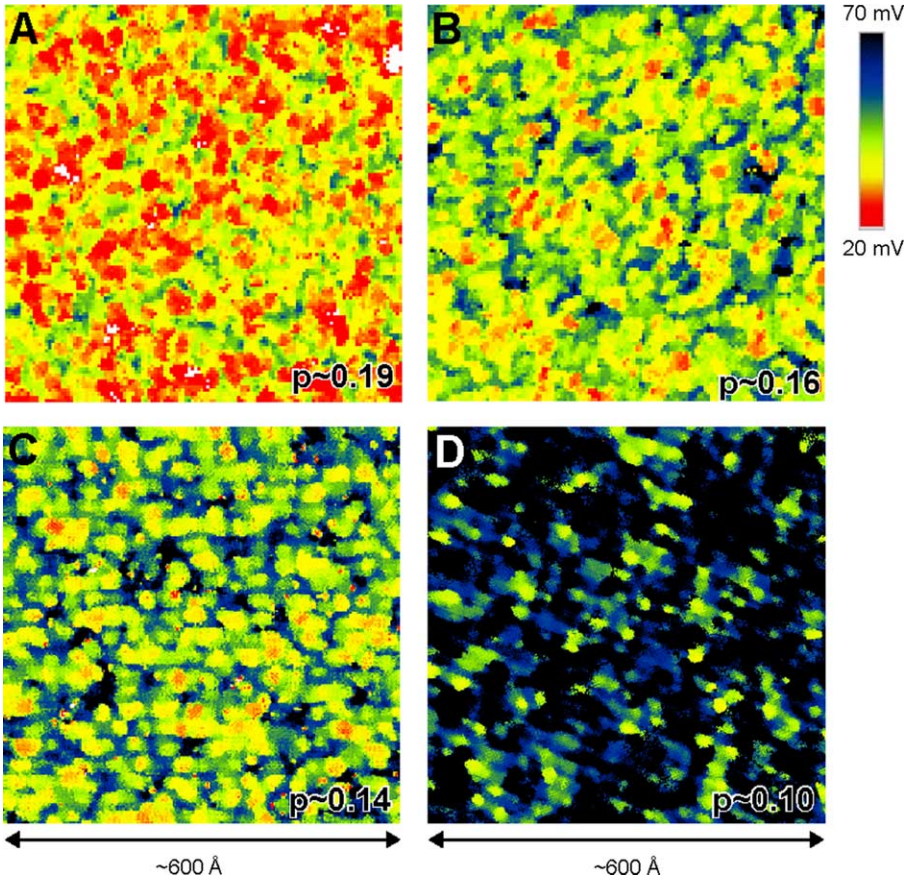

Fig. 5. Gap maps of 60 nm square regions of Bi-2212 showing nanoscale electronic disorder. (A) Sample doping 0.19; (B) 0.16; (C) 0.14; (D) 0.10. The color scale on the right represents Δ in all panels. As the doping decrease, more and more darker (larger Δ) regions appear.

these data within a scattering-induced quasiparticle interference model [16], the $\vec{q}$-vectors can be consistent [10] within the Fermi-surface and energy gap pictures in agreement with photoemission studies [17] of $d_{x^2-y^2}$ cuprate superconductors. Namely, elastic scattering occurs between the points of high joint density of states at a given energy (red dots), leading to a set of specific interference $\vec{q}$-vectors responsible for the observed standing waves, as shown in Fig. 4C. Most likely scattering centers responsible for these modulations are related to weak scattering potentials from out-of-plane dopant atoms [18].

6. Nanoscale electronic disorder in $\Delta(\vec{r})$

Doping dependence of gap maps or $\Delta(\vec{r})$ [12,13] shows disorder of another kind. Fig. 5 shows $\Delta(\vec{r})$ maps of $Bi_2Sr_2CaCu_2O_{8+x}$ in a 60×60 nm *FOV* at dopings ranging from $\sim$0.19 to $\sim$0.1. The identical color scale is used for the Δ values in all four gap-maps. These gap-maps reveal intense electronic disorder, and the gap values range from 20 meV to over 70 meV, with $\sim$3 nm big domain-like area of the same Δ value. The mean gap value rises as the doping falls, in agreement with other probes [15]. All the regions in these disordered images share the same low energy quasiparticles as judged from FT-STS studies [19]. These effects were completely unexpected. By now they have been widely observed [8,10,12,13,20–23]. The source of these electronic disorder phenomena in cuprates is still unknown. To tackle these critical issues, SI-STM studies of the electronic disorder and dopant atom disorder, and their correlations are currently underway.

7. 'Checkerboard' states in vortex core and underdoped region

The STM study of the electronic structure of the cuprate vortex core [11] initiated the interest of the 'checkerboard' states which recently became the focus of much theoretical research on under-doped cuprates [24–34]. It was shown that the pseudogap-like conductance spectrum-V shaped spectra without coherence peaks—in the vicinity of the vortex core of the $Bi_2Sr_2CaCu_2O_{8+x}$ (Fig. 6A) appear with a checkerboard incommensurate low energy LDOS modulations with associated $\vec{q}$ vectors of $(\pm2\pi/4.3a_0,0)$, $(0\pm2\pi/4.3a_0)\pm15\%$ (Fig. 6B) The $\sim4a_0$ periodicity in the direction of the Cu–O bonding of the vortex-induced LDOS modulations are believed to be caused by a electronic phase which can become stabilized at the vortex cores when high-T_C superconductivity is suppressed. This discovery is very important because it shows one can access the unknown non-superconducting state in high-T_C cuprates by suppressing the superconductivity near the vortex core,

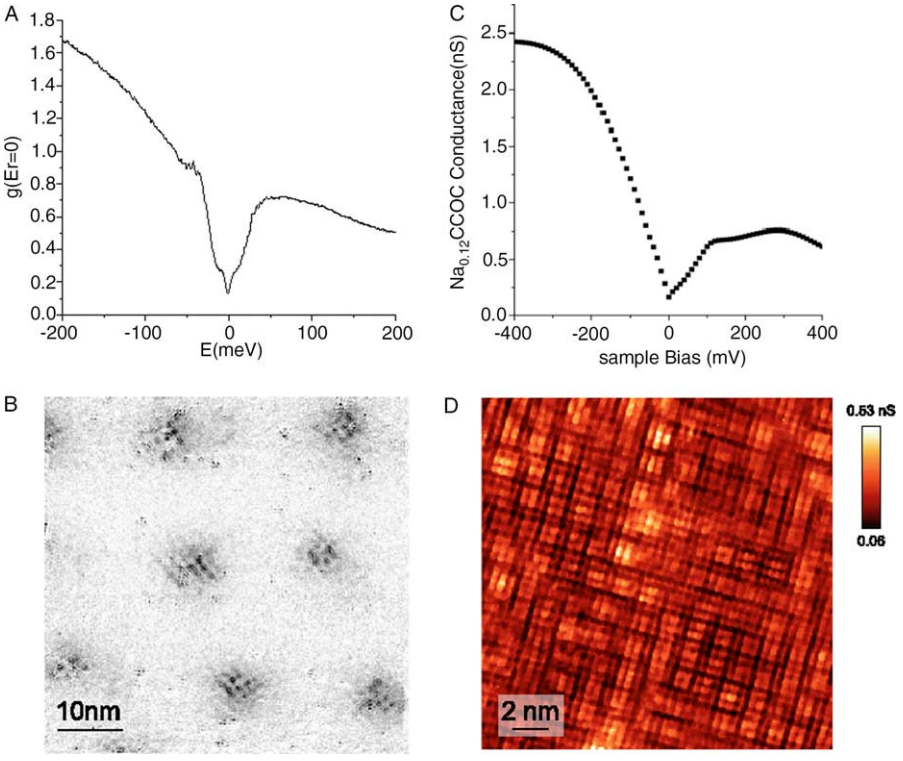

Fig. 6. (A) A local density of states (LDOS) spectrum at vortex center in $Bi_2Sr_2CaCu_2O_{8+x}$. (B) Map of the additional states produced by the field [11]. (C) A differential conductance spectrum on $Ca_{2-x}Na_xCuO_2Cl_2$. D. A map of the density of states at 24 meV [35]. In both cases the modulations are aligned with Cu–O bond directions.

and also shows clear checkerboard electronic crystal characteristics. The natural question to follow is, therefore, 'Is the checkerboard state a precursor to the high-T_C superconducting phase?' Recently, a possibly related checkerboard modulation in LDOS is observed in strongly underdoped $Bi_2Sr_2CaCu_2O_{8+x}$ [19].

To get around the nanoscale disorder of $Bi_2Sr_2CaCu_2O_{8+x}$, we chose another member of high-T_C cuprate family to study. $Ca_{2-x}Na_xCuO_2Cl_2$ is high-T_C superconductor, whose parent material $Ca_2CuO_2Cl_2$ is a canonical Mott insulator [35]. We have studied this $Ca_{2-x}Na_xCuO_2Cl_2$ at the doping level from $8\%(T_C=0)<x<12\%(T_C=20\ \mathrm{K})$, with the SI-STM technique we described in previous sections. Below about 100 mV, a V-shaped energy gap around the Fermi level emerges in the LDOS, as shown in Fig. 6C. This gap is particle-hole symmetric, and within the gap, strong non-dispersive electronic modulations of an exact commensurate $4a_0\times4a_0$ checkerboard are observed (Fig. 6D). We observed this phenomena throughout the doping range studied. This discovery is also consistent with a crystalline electronic state existing at low hole doping in the zero temperature pseudogap regime of $Bi_2Sr_2CaCu_2O_{8+x}$ [19]. This checkerboard electronic crystal may be a new precursor phase between the Mott insulating phase and the superconductivity.

8. Conclusions

Due to the novel spectroscopic imaging STM (SI-STM) techniques, numerous unexpected atomic scale electronic structures have been brought to light. Among these significant discoveries are nanoscale gap disorder, quasiparticle interference modulation and 'checkerboard' states. Also, the effects of dopant atoms on the nanoscale disorder, and the relation of the checkerboard state to the superconductivity have become new foci of interest in macroscopic quantum physics of high-T_C cuprates.

Acknowledgements

JCD wishes to acknowledge and thank collaborators: K. McElroy, C. Lupien, D.-H. Lee, H. Eisaki, T. Hanaguri, E.W. Hudson, J.E. Hoffman, Y. Kohsaka,, K.M. Lang, V. Madhavan, R.W. Simmonds, H. Takagi, and S. Uchida. This work has been supported by the Office of Naval Research under grant N00014-03-1-0674, by the National Science Foundation under grants DMR-9971502 and NSF-ITR FDP-0205641, by Grant-in-Aid for Scientific Research on Priority Area, by a COE Grant from the Ministry of Education (Japan), by support from NEDO (Japan) and by Cornell University.

References

[1] J.R. Schrieffer, Theory of Superconductivity, Addison-Wesley, New York, 1983.
[2] S.H. Pan, E.W. Hudson, J.C. Davis, Rev. Sci. Instrum. 70 (1999) 1459.
[3] H. Eisaki, N. Kaneko, D.L. Feng, A. Damascelli, P.K. Mang, K.M. Shen, Z.-X. Shen,, M. Greven, Phys. Rev. B 69 (2004) 064512.
[4] D.J.V. Harlingen, Rev. Mod. Phys. 67 (1995) 515.
[5] C.C. Tsuei, J.R. Kirtley, Rev. Mod. Phys. 72 (2000) 969.
[6] J.L. Tallon, J.W. Loram, Physica C 349 (2001) 53.
[7] E. Hudson, S.H. Pan, A.K. Gupta, K.W. Ng, J.C. Davis, Science 285 (1999) 88.
[8] V. Madhavan, K.M. Lang, E.W. Hudson, S.H. Pan, H. Eisaki, S. Uchida, J.C. Davis, Bull. Am. Phys. Soc. 45 (2000) 416.
[9] J.E. Hoffman, K. McElroy, D.H. Lee, K.M. Lang, H. Eisaki, S. Uchida, J.C. Davis, Science 297 (2002) 1148.
[10] K. McElroy, R.W. Simmonds, J.E. Hoffman, D.H. Lee, J. Orenstein, H. Eisaki, S. Uchida, J.C. Davis, Nature 422 (2003) 592.
[11] J.E. Hoffman, E.W. Hudson, K.M. Lang, V. Madhavan, H. Eisaki, S. Uchida, J.C. Davis, Science 295 (2002) 466.
[12] S.H. Pan, J.P. O'Neal, R.L. Badzey, C. Chamon, H. Ding, J.R. Engelbrecht, Z. Wang, H. Eisaki, S. Uchida, A.K. Gupta, K.-W. Ng, E.W. Hudson, K.M. Lang, J.C. Davis, Nature 413 (2001) 282.
[13] K.M. Lang, V. Madhavan, J.E. Hoffman, E.W. Hudson, H. Eisaki, S. Uchida, J.C. Davis, Nature 415 (2002) 412.
[14] Y. Gao, P. Lee, P. Coppens, M.A. Subramanian, A.W. Sleight, Science 241 (1988) 954.
[15] A. Damascelli, Z. Hussain, Z.X. Shen, Rev. Mod. Phys. 75 (2003) 473.
[16] Q.H. Wang, D.H. Lee, Phys. Rev. B 67 (2003) 020511.
[17] H. Ding, M.R. Norman, J.C. Campuzano, M. Randeria, A.F. Bellman, T. Yokoya, T. Takahashi, T. Mochiku, K. Kadowaki, Phys. Rev. B 54.
[18] D.J. Scalapino, T.S. Nunner, P.J. Hirschfeld, cond-mat/0409204.
[19] K. McElroy, D.-H. Lee, J.E. Hoffman, K.M. Lang, J. Lee, E.W. Hudson, H. Eisaki, S. Uchida, J. Davis, cond-mat/0406491, to appear in Phys. Rev. Lett., 2005.
[20] C. Howald, P. Fournier, A. Kapitulnik, Phys. Rev. B 64 (2001) 100504.
[21] T. Cren, D. Roditchev, W. Sacks, J. Klein, Europhys. Lett. 54 (2001) 84.
[22] A. Matsuda, S. Sugita, T. Fujii, T. Watanabe, J. Phys. Chem. Solids 62 (2001) 65.
[23] G. Kinoda, T. Hasegawa, S. Nakao, T. Hanaguri, K. Kitazawa, K. Shimizu, J. Shimoyama, K. Kishio, Phys. Rev. B 67 (2003) 224509.
[24] M. Vojta, Phys. Rev. B 66 (2002) 104505.
[25] H.D. Chen, J.P. Hu, S. Capponi, E. Arrigoni, S.C. Zhang, Phys. Rev. Lett. 89 (2003) 137004.
[26] C. Howald, H. Eisaki, N. Kaneko, M. Greven, A. Kapitulnik, Phys. Rev. B 67 (2003) 014533.
[27] A.S. Mishchenko, N. Nagaosa, Phys. Rev. Lett. 93 (2004) 036402.
[28] H.D. Chen, O. Vafek, A. Yazdani, S.C. Zhang, Phys. Rev. Lett. 93 (2004) 187002.
[29] P.W. Anderson, cond-mat/0406038.
[30] E. Kaneshita, I. Martin, A.R. Bishop, condmat/0406042.
[31] A.S. Alexandrov, cond-mat/0407401.
[32] L. Balents, L. Bartosch, A. Burkov, S. Sachdev, K. Sengupta, cond-mat/0408329.
[33] H.X. Huang, Y.Q. Li, F.C. Zhang, condmat/0408504.
[34] A. Ghosal, A. Kopp, S. Chakravarty, condmat/0412241.
[35] T. Hanaguri, C. Lupien, Y. Kohsaka, D.-H. Lee, M. Azuma, M. Takano, H. Takagi, J.C. Davis, Nature 430 (2004) 1001.